Annals of Physics 470 (2024) 169807

Contents lists available at ScienceDirect

Annals of Physics

journal homepage: www.elsevier.com/locate/aop

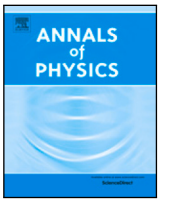

Phases and coherence of strongly interacting finite bosonic systems in shallow optical lattice

Subhrajyoti Roy [a], Rhombik Roy [b,1], Arnaldo Gammal [c], Barnali Chakrabarti [b,c,*], Budhaditya Chatterjee [d]

[a] Indian Statistical Institute, Tezpur, 784501, Assam, India
[b] Department of Physics, Presidency University, 86/1 College Street, Kolkata, 700073, West Bengal, India
[c] Instituto de Física, Universidade de Sao Paulo, Sao Paulo, 05508-090, Brazil
[d] Department of Physics, Asansol Girls' College, Asansol, 713304, West Bengal, India

ARTICLE INFO

Keywords:
Many-body coherence
Shallow optical lattice
MCTDHB

ABSTRACT

We explore the ground states of strongly interacting bosons in the vanishingly small and weak lattices using the multiconfiguration time-dependent Hartree method for bosons (MCTDHB) which calculate numerically exact many-body wave function. Two new many-body phases: fragmented or quasi superfluid (QSF) and incomplete fragmented Mott or quasi Mott insulator (QMI) are emerged due to the strong interplay between short-range contact interaction and lattice depth. Fragmentation is utilized as a figure of merit to distinguish these two new phases. We utilize the eigenvalues of the reduced one-body density matrix and define an order parameter that characterizes the pathway from a very weak lattice to a deep lattice. We provide a detailed investigation through the measures of one- and two-body correlations and information entropy. We find that the structures in one- and two-body coherence are good markers to understand the gradual built-up of intra-well correlation and decay of inter-well correlation with increase in lattice depth. For the dipolar interaction, the many-body features become more distinct and true Mott state can appear even in a shallow lattice. Whereas, for incommensurate fraction of particles, incomplete localization happens that exhibits distinct features in the measure of two-body coherence.

1. Introduction

Ultracold atomic gases provide unprecedented experimental control to study complex many-body systems in lattice [1–3]. Experimentally it is quite straightforward to tune the lattice depth of the periodic optical potential and subsequent study of different phases of ultracold atoms [4–7] The interplay between the lattice depth and interatomic interaction triggers the superfluid-to-insulator transition commonly known as Mott transition [6,8,9]. The Mott transition takes place in deep lattice which is characterized by a high localization of the atoms and theoretically the Bose-Hubbard (BH) model essentially captures the underlying process [10]. Later, many different extensions of the standard BH model have been introduced, specially when interatomic interactions are strong enough which leads to interesting phenomenon [11]. Nevertheless, there are open questions on the validity of BH model for ultracold gases in shallow lattice. In many aspects, the experiments with ultracold atoms in shallow lattice are easily realized. In Refs. [12,13], amplitude of the periodic optical potential is varied from zero to large value and the Mott transition in the shallow lattice has been

* Corresponding author at: Department of Physics, Presidency University, 86/1 College Street, Kolkata, 700073, West Bengal, India.
E-mail address: barnali.physics@presiuniv.ac.in (B. Chakrabarti).
[1] Current affiliation: Department of Physics, University of Haifa, 3498838 Haifa, Israel.

https://doi.org/10.1016/j.aop.2024.169807
Received 21 March 2024; Accepted 13 September 2024
Available online 17 September 2024

observed by modulation spectroscopy and transport measurements. The pinning transition in the vanishing lattice is described by (1+1) quantum sine–Gordon model [14]. Later, complete phase diagram of the continuous model is mapped out [15–18] and it is demonstrated that the sine–Gordon model used for shallow lattice is insufficient.

In the present work, we address the system implemented in the experiment [12], one dimensional strongly interacting bosons in optical lattice of variable strength. The main purpose of the work is to understand the correlation of the strongly interacting few bosons system in vanishing lattice utilizing numerically exact solution of Schrödinger equation. The study of strong quantum correlation in a smaller system with a very finite number of interacting particles are receiving special interest in the recent experiments [19,20]. We use the multiconfigurational time-dependent Hartree method for bosons (MCTDHB) [21–27], implemented in the MCTDH-X software [28,29].

We observe strong competition between the dimensional confinement and quantum correlation. We find the emergent phases for strongly interacting bosons in extremely weak lattice are neither the ideal superfluid (SF) nor the ideal Mott (MI) phases. In the limit of shallow potential, when the lattice effect is subrelevent, many-body phases are organized and controlled by the quantum correlation originated from strong interatomic interaction. The many-body physics of such strongly correlated system lies beyond the scope of BH model [9,30]. We utilize 'fragmentation' as the key measure to distinguish the emergent phases. We quantify "excited fragmentation" as the fraction of atoms contributed by the other natural orbitals except the one with the largest occupation. Fragmentation is the hallmark of MCTDHB which utilizes multiorbitals ansatz and the strongly interacting bosons may be fragmented even in a very weak or vanishingly small lattice.

The present work provides a complete path for varying lattice depth $V_0 = 0.1E_r$ to $8.0E_r$, for fixed inter-atomic interaction which corresponds to strongly interacting repulsive bosons. We follow the zero temperature phase diagram of the continuous model of Ref. [17]. The critical value of Lieb Liniger parameter at the vanishing lattice is $\gamma_c = 3.65$. The effective coupling constant of Lieb Liniger model (γ) is related to the two-body interaction strength (λ_0) by $\gamma = \frac{m\lambda_0}{\hbar^2 n}$, where $n = \frac{N}{L}$ is the density of the gas and L is the length of the system. We obtain $\lambda_0 = 1.05$ which corresponds to critical value of Lieb Liniger parameter in the vanishing lattice. To observe how the competition between the lattice depth and interatomic interaction affect the inter-well correlation in shallow lattice, we keep λ_0 fixed in the entire calculation. We extract one-body and two-body correlations utilizing numerically exact many-body wave function. The system consists of $N = 3$ strongly interacting bosons in $S = 3$ three lattice sites. This elemental building block is able to capture all essential many-body physics in the larger lattice. In our small ensemble, the term 'quantum phase' is not rigorously applicable. However, the calculated many-body states can be taken as few-body precursor of thermodynamic phases. For clarity we term the few-body states as 'phase'. The two key measures : fragmentation and Glauber correlation functions are utilized to describe the highly correlated phases in varying lattice depth. For almost vanishing lattice ($V_0 \simeq 0.5E_r$); several natural orbitals have significant population; thus the many-body phase is fragmented. It also exhibits strong diagonal correlation and weak off-diagonal correlation in one-body and clear signature of anti-bunching effect in two-body correlations. It is not a SF phase which is designated by macroscopic occupation in one single orbital and uniform global correlation across the lattice. It is also not a Mott phase as it does not exhibit complete localization in each well. Quantitative measures as discussed in the result section establish that the many-body phase is best diagnosed as fragmented superfluid or quasi SF (QSF) phase. For weak lattice ($V_0 \simeq 2.0E_r$); the system becomes more fragmented but does not exhibit S-fold fragmentation. The diagonal correlation in one-body becomes stronger at the cost of weaker off-diagonal correlation. So the many-body phase is close to Mott but not a perfect Mott. The quantitative estimates establish that the many-body phase can be designated as incomplete fragmented Mott or quasi-Mott (QMI) phase. For larger lattice depth ($V_0 \simeq 8.0E_r$), completely fragmented Mott phase is achieved.

We repeat the calculation with long-range dipolar interaction, Eq. (3) with $g_d = 1.05$. The long-range tail of the dipolar interaction enhances the fragmentation and the strongly interacting dipolar superfluid is more fragmented and correlated compared to the contact interaction. The dipolar interaction does not lead to any new phases, the quasi superfluid and quasi Mott phases exhibit strong intra-well correlation. The transition from quasi SF to quasi Mott and fully fragmented Mott in deep lattice happens very fast.

We also study the phases for shallow incommensurate lattice which is more susceptible to the case of commensurate lattice having exact number of particles compared to the number of wells. For filling factor $\nu = \frac{N}{S} < 1$, there will always be a delocalized fraction of particles and on-site interaction effect is not manifested due to low population. For $\nu > 1$, the extra delocalized particles sit on the commensurate background of localized particles. Both cases of incommensurate lattice features rich many-body correlation.

The quasi-many-body phases and correlations are studied by the key quantities: (a) occupation in natural orbital, (b) excited fragmentation, (c) order parameter (d) delocalization in Fock space (e) one-body and two-body correlations and (f) information entropy measures. All these measures are synchronized and clearly define the many-body phases in vanishing to weak to deep lattices. We observe that in the shallow lattice, the quasi many-body phases are always fragmented which is beyond the scope of mean-field theory and Bose-Hubbard model. The inter-well and intra-well correlation are the possible measures which can be experimentally determined in the set up of very weak lattice.

The paper is organized as follows. In Section 2, we introduce the theoretical framework. Section 3 introduces the quantities of interest. In Section 4, we present the results. Section 5 concludes our observations.

2. System and method

For N bosons in a quasi-one-dimensional optical lattice, the Hamiltonian is

$$\hat{H} = \sum_{i=1}^{N} \hat{h}(x_i) + \sum_{i<j=1}^{N} W(x_i - x_j) \tag{1}$$

$\hat{h}(x) = \hat{T}(x) + \hat{V}_{trap}(x)$ is the one-body Hamiltonian. $\hat{T}(x)$ is the kinetic energy operator; $\hat{T}(x) = -\frac{1}{2}\sum_{i=1}^{N}\frac{\partial^2}{\partial x^2}$ and $\hat{V}_{trap}(x)$ is the external trapping potential. $V_{trap}(x) = V_0 \sin^2(kx)$. V_0 is the depth of the potential and k is the wave vector. $W(x_i - x_j)$ is the two-body interaction potential. For contact interaction

$$W(x_i - x_j) = \lambda_0 \delta(x_i - x_j) \tag{2}$$

where λ_0 is the interaction strength determined by the scattering length and the transverse confinement frequency. For the long-ranged dipolar interaction

$$W(x_i - x_j) = \frac{g_d}{|x_i - x_j|^3 + \alpha_0} \tag{3}$$

g_d is the pure dipolar interaction strength; $g_d = \frac{d_m^2}{4\pi\epsilon_0}$ for electric dipoles and $g_d = \frac{d_m^2\mu_0}{4\pi}$ for magnetic dipoles, d_m being the dipole moment, ϵ_0 is the vacuum permittivity, and μ_0 is the vacuum permeability. α_0 is the short-range cutoff to avoid singularity at $x_i = x_j$. We choose the cut-off parameter such that the effective interaction $V_{\text{eff}} = \int_D \frac{g_d}{x^3+\alpha_0}\mathrm{d}x = \int_D \delta(x)\mathrm{d}x = 1$, where the $D = [-4.71, 4.71]$ encompasses the entire simulation domain. We consider three lattice sites with periodic boundary conditions, the strong transverse confinement ensures a quasi-1D trap. We choose strong repulsive interaction of strength $\lambda_0 = g_d = 1.05$ for the entire simulation. We rescaled the Hamiltonian by the lattice recoil energy $E_r = \frac{\hbar^2 k^2}{2m}$ to achieve the convenient dimensionless units; $\hbar = m = k = 1$. The scaled triple well potential is given by $V_{trap}(x) = V_0 \sin^2 x$. The length and time units are given in terms of k^{-1} and $\frac{\hbar}{E_r}$ respectively. All quantities are in dimensionless units throughout.

The MCTDHB method represents a bosonic variant within the broader family of MCTDH methodologies [31–40] in which, the many-body wavefunction is constructed as a linear combinations of the time dependent permanents and time-dependent complex-valued coefficients,

$$|\psi(t)\rangle = \sum_{\vec{n}} C_{\vec{n}}(t)|\vec{n};t\rangle, \tag{4}$$

where

$$|\vec{n};t\rangle = |n_1, n_2, \ldots, n_M; t\rangle = \prod_{i=1}^{M}\left[\frac{(b_i^\dagger(t))^{n_i}}{\sqrt{n_i!}}\right]|\text{vac}\rangle. \tag{5}$$

Each operator $b_k^\dagger(t)$ creates a boson occupying the time-dependent single-particle state (orbital) $\phi_k(x,t)$. Note that the expansion coefficients $\{C_{\vec{n}}(t)\}$ as well as orbitals $\{\phi_i(x,t)\}_{i=1}^{M}$ that build up the permanents $|\vec{n};t\rangle$ are explicitly time dependent and fully variationally optimized quantities [22,24]. For N bosons distributed over M orbitals, the number of permanents become $N_{conf} = \begin{pmatrix} N+M-1 \\ N \end{pmatrix}$. Thus, in the limit of $M \to \infty$, the wave function becomes exact, and the set $|n_1, n_2, \ldots, n_M\rangle$ spans the complete N-particle Hilbert space. For practical calculation, we restrict the number of orbitals to the desired value requiring the proper convergence in the measured quantities. Compared to a time-independent basis, as the permanents are time-dependent, a given degree of accuracy is reached with much shorter expansion [41,42]. We also emphasize that MCTDHB is more accurate than exact diagonalization which uses the finite basis and is not optimized. Whereas in MCTDHB, as we use a time adaptive many-body basis set, it can dynamically follow the building correlation due to inter-particle interaction [23,24,43,44] and it has been widely used in different theoretical calculations [45–51]. To get the ground state, we propagate the MCTDHB equations in imaginary time. As in the shallow lattice, the many-body wavefunction shows strong fragmentation—we discuss the issue of convergence of simulation with MCTDHB. The convergence is ascertained in the following ways. We systematically increase the number of orbitals until the basic measures like occupation in natural orbitals and degree of fragmentation converge. Additionally, the convergence is further confirmed when the occupation in the highest orbital is negligible.

3. Quantity of Interest

3.1. Natural occupation and excited fragmentation

Natural occupation and the excited fragmentation are the two key measures to understand the transition from QSF to QMI to MI with increase in lattice depth. Excited fragmentation is defined as the fraction of atoms that do not occupy the lowest eigenstate of the reduced one-body density matrix or the contribution coming from other orbitals except the one that is maximally populated. The reduced one-body density matrix is

$$\rho^{(1)}(x,x') = \sum_k \rho_k^{(NO)}\phi_k^{*(NO)}(x)\phi_k^{(NO)}(x'). \tag{6}$$

$\phi_k^{(NO)}(x)$ are the eigenfunctions of $\rho^{(1)}$ and known as natural orbitals. $\rho_k^{(NO)}$ are the eigenvalues of $\rho^{(1)}$ and known as natural occupations. In the mean-field perspective, when one single natural orbital is occupied, $\rho^{(1)}$ has only a single macroscopic eigenvalue, and the many-body state is non-fragmented. The excited fragmentation (F) becomes zero. However multi-orbital ansatz facilitates to study of the beyond mean field picture-several natural orbitals may exhibit significant population and F may become non-zero. The corresponding state is fragmented.

3.2. Order parameter

We define an order parameter

$$\triangle = \sum_i \left(\frac{n_i}{N}\right)^2 \tag{7}$$

where n_i is the natural occupation in ith orbital. For the SF phase, $\triangle = 1$ and only one eigenvalue is nonzero. For the Mott phase, the number of significantly contributing orbitals becomes equal to the number of sites in the lattice, and $\triangle = \frac{1}{S}$, S is the number of lattice sites. Thus $\triangle = 1$ and $\triangle = \frac{1}{S}$ are the two extreme values for the two known phases. We find $\triangle$ is a good marker to identify the QSF and QMI phases in the shallow lattice.

3.3. Glauber correlation function

Understanding a quantum many-body phase implies understanding the role of correlations. For a strongly interacting system, correlation functions of higher orders are necessary to understand the complex phases. The pth order Glauber correlation function $g^{(p)}(x_1', \ldots, x_p', x_1, \ldots, x_p; t)$ measures degree of spatial coherence and correlations within the system. It is defined as:

$$g^{(p)}(x_1', \ldots, x_p', x_1, \ldots, x_p) = \frac{\rho^{(p)}(x_1, \ldots, x_p | x_1', \ldots, x_p')}{\sqrt{\prod_{i=1}^{p} \rho^{(1)}(x_i|x_i)\rho^{(1)}(x_i'|x_i')}}. \tag{8}$$

where $\rho^{(p)}(x_1', \ldots, x_p'|x_1, \ldots, x_p)$ is the pth order reduced density matrix and describes the joint probability distribution of finding p particles at specific positions and defined as

$$\rho^{(p)}(x_1', \ldots, x_p'|x_1, \ldots, x_p) = \frac{N!}{(N-p)!} \int dx_{p+1}, \ldots, dx_N \psi^*(x_1', \ldots, x_p', x_{p+1}, \ldots, x_N)\psi(x_1, \ldots, x_p, x_{p+1} \ldots, x_N). \tag{9}$$

The diagonal elements of $g^{(p)}(x_1', \ldots, x_p', x_1, \ldots, x_p)$, denoted as $g^{(p)}(x_1, \ldots, x_p)$, provide a measure of pth order coherence. If $|g^{(p)}(x_1, \ldots, x_p)| = 1$, the system is fully coherent, while deviations from unity indicate partial coherence. Specifically, $g^{(p)}(x_1, \ldots, x_p) > 1$ implies correlated detection probabilities at positions $x_1, \ldots, x_p$, while $g^{(p)}(x_1, \ldots, x_p) < 1$ indicates anti-correlations. These measures collectively provide valuable insights into the evolving density profile, coherence and are especially useful to understand the interplay between inter-well and intra-well correlations.

3.4. Many-body entropy

We employ the measures of information entropy as another marker to understand the pathway from QSF to QMI and finally to the MI phase. In general, the Shannon information entropy calculated from one-body density is chosen as the ideal quantity to establish a universal relation between entropy and the number of interacting particles for diverse systems like atoms, nuclei and clusters [52–54]. However for strongly correlated bosons, measures of Shannon information entropy are insufficient as they are insensitive to interatomic correlation that is present in the many-body state. In the shallow lattice, as several natural orbitals exhibit significant population, we define an equivalent measure of information entropy called occupation entropy or number entropy.

$$S_n = -\sum_i n_i [\ln n_i]. \tag{10}$$

S_n is an entropy obtained from the natural occupation. For the Gross Pitaevskii mean-field theory, $S_n = 0$ always as there is only one natural occupation $\vec{n}_1 = \frac{n_1}{N} = 1$. For multi-orbital theories, several occupation numbers can be different from 0, and the magnitude of S_n indicates how well the state could be described by a mean-field approach. In the SF phase, a single orbital is sufficient to describe the state, resulting S_n equals to zero. Conversely, in the Mott insulator phase, the system becomes S-fold fragmented, S_n will exhibit non-zero values. We utilize the Gaussian Orthogonal Ensemble (GOE) theory for comparative analysis [44,55,56]. Thus, during the transition from the SF to MI phase, S_n makes a transition from nonzero minimum value to the GOE value, facilitating the detection of intermediate phases such as quasi-superfluid (QSF) and quasi-Mott insulator (QMI). For long range dipolar interaction, the system is already in a maximally fragmented state, initially S_n is larger than GOE prediction and with increase in lattice depth S_n gradually decreases to reach to GOE prediction.

4. Results

4.1. Fragmentation and order parameter

Our set up consists of $N = 3$ bosons in triple well set up $S = 3$ with periodic boundary condition. Interaction strength is fixed to $\lambda_0 = 1.05$ for contact interaction and $g_d = 1.05$ for dipolar interaction. We run simulations with 512 grid points in an interval $x\epsilon\{-\frac{3\pi}{2}, +\frac{3\pi}{2}\}$. We fix the number of orbitals to $M = 9$ both for contact interaction and dipolar interaction, when the occupation in the last orbital becomes insignificant. We have also validated the convergence of our calculations by repeating the computations with $M = 12$ orbitals, consistently yielding identical results for the measured quantities. A detail calculation for convergence is provided in Appendix. We demonstrate how the natural populations in different orbitals are used to construct the mesoscopic "order parameter".

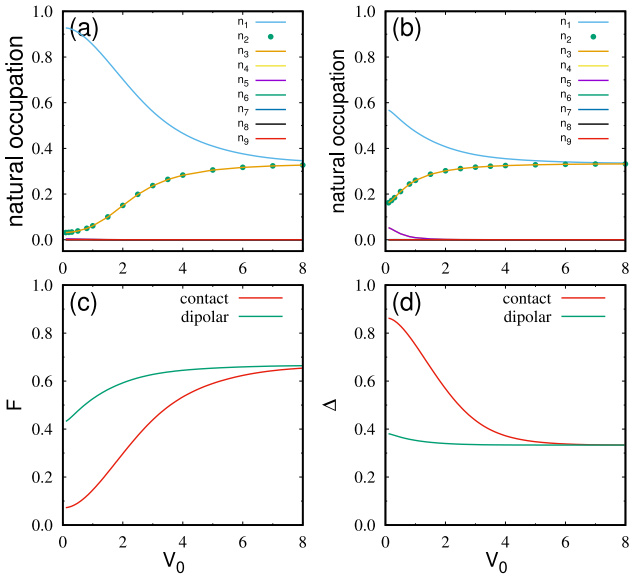

Fig. 1. (a) Natural occupations for contact interaction with $M = 9$ orbitals. (b) Natural occupations for dipolar interaction with $M = 9$ orbitals. (c) Fraction of atoms outside the natural orbital having maximum occupation. (d) Order parameter, all as a function of lattice depth V_0 and for fixed interaction strength $\lambda_0 = g_d = 1.05$, three interacting bosons in three wells. The emergence of fragmentation and subsequent growth in fragmentation, signify that the system enters a strongly correlated phase with increase in lattice depth. All quantities are dimensionless, see text for additional details.

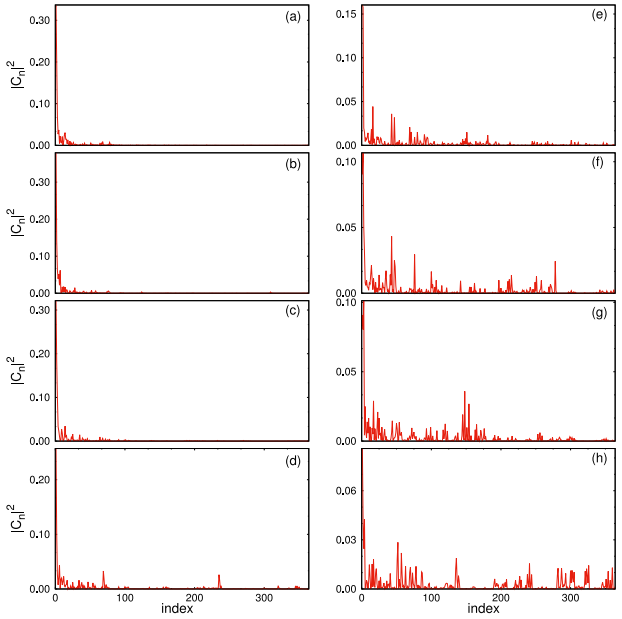

Fig. 2. Delocalization in Fock space in the fragmented SF (QSF) and incomplete fragmented MI (QMI) states. The distribution of the magnitude of the coefficients is shown as a function of the index for the choice of V_0(in the unit of E_r) $= 0.3, 0.5, 1.0, 2.0$. The left column corresponds to the contact interaction and the right column corresponds to dipolar interaction. The transition from QSF to QMI is exhibited by the transition from partial delocalization to complete delocalization in Fock space. All quantities are dimensionless.

The concept of order parameter is generally used in the thermodynamic limit. However, for our choice of a small ensemble, the ground state properties that are presented here are analogous to the macroscopic phases. The few-body physics remains the same with five bosons in five wells. Thus "order parameter" can be taken as a finite-sized precursor of the quantum phases.

Figs. 1(a), 1(b) show the plots of the eigenvalues $\rho_k^{(NO)}$ for contact and dipolar interaction respectively. In both cases, orbital occupations are plotted for $M = 9$ orbitals. We need to mention here that $M = 9$ orbitals are sufficient to demonstrate well converged results for contact interaction as well as for dipolar interaction. For contact interaction (Fig. 1(a)), only the first three orbitals

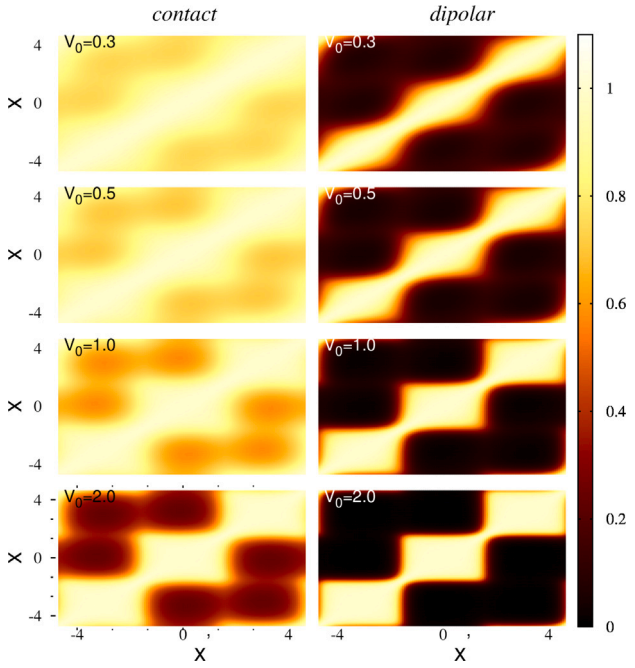

Fig. 3. First-order coherence of the fragmented SF (QSF), incomplete fragmented MI (QMI) states. The normalized first-order correlation function $|g^{(1)}(x,x')|^2$ is plotted for various lattice depth. The left column corresponds to contact interaction and the right column corresponds to dipolar interaction. For the fragmented SF phase with contact interaction, in the vanishingly small lattice, structureless diagonal correlation, as well as off-diagonal correlation, are exhibited. Whereas for dipolar interaction, strong diagonal correlation and lattice structure are seen, the vanishing off-diagonal correlation demonstrates localization even in such weak lattice. With the increase in the lattice depth, the lattice effect and interatomic interaction compete and result in incomplete fragmented Mott (QMI). The structure in the diagonal line develops, but the off-diagonal correlation is not completely lost for contact interaction. For dipolar interaction the correlation function is characterized by three distinct Mott lobes with $|g^{(1)}|^2 \simeq 1$ along the diagonal and $|g^{(1)}|^2 \simeq 0$ on the off-diagonal. Thus, the first-order coherence is maintained within wells and completely lost between the wells. All quantities are dimensionless.

$\left(\rho_1^{(NO)}, \rho_2^{(NO)}, \rho_3^{(NO)}\right)$ exhibit significant contribution for the entire simulation. Initially for almost vanishing lattice ($V_0 = 0.1E_r$), the lowest orbital has close to 90% population, and the other two orbitals contribute close to 5% (each). So the state is not a superfluid with configuration. However, as the population in the first natural orbital is significantly high compared to the two other orbitals, we call it fragmented SF or QSF. With an increase in lattice depth, V_0, the occupation of the first natural orbital gradually decreases, and that in the second and third natural orbitals increases which leads to complete three-fold fragmentation for deep lattice ($V_0 = 8.0E_r$). In weak lattice, the many-body state is not exactly three-fold fragmented, but the population imbalance in the lowest three orbitals is minimum, we call it the incomplete fragmented Mott phase (QMI). At deep lattice three-fold fragmentation is described by 33.3% population of each three lowest orbitals, it is the unique feature of the MI phase. Thus strongly interacting bosons in shallow lattices exhibit two new many-body phases, termed QSF and QMI. They are the *hallmark* states of MCTDHB and beyond the scope of any other existing model calculations. These QSF and QMI states can be distinguished from SF and MI states by the measures of one-body and two-body Glauber correlation functions. For dipolar interaction, (Fig. 1(b)), the dipolar bosons are strongly fragmented with close to 60% population in the first orbital and 15% population in the second and third orbitals. We also find small contribution from the fourth and fifth orbital. The many-body state is strongly fragmented superfluid. With increase in lattice depth, population in the second and third orbitals increase at the cost of reduction in population in the first orbital. Compared to the contact interaction, three-fold fragmented Mott state is achieved close to $V_0 = 6.0E_r$.

We quantify the degree of fragmentation by introducing excited fragmentation (F). F determines the fraction of atoms that are outside the natural orbital of the highest population. In Fig. 1(c), we plot F as a function of varied lattice depth. As $F > 0$ for the entire range of lattice depth, the system is always fragmented. With the increase in V_0, fragmentation increases, and at the deep lattice, it saturates to 0.66 which refers to a three-fold fragmented Mott localization and can be configured as a number state $|1,1,1\rangle$. For dipolar interaction fragmentation is always higher than that for contact interaction and quickly saturates to 0.66. To get more insight into the fragmented SF and non-fragmented Mott phase, we introduce an order parameter (Eq. (7)). In Fig. 1(d), we plot $\triangle$ for various lattice depth potentials. The two extreme limits are 1.0 for SF and $\frac{1}{S}$=0.33 for true MI states. The order parameter does not coincide with the SF or MI phases for vanishingly small and weak lattices. Fig. 1(d) clearly exhibits that the order parameter scales QSF to QMI to MI phases. For strongly fragmented dipolar superfluid the order parameter smoothly translated from QSF in the vanishing lattice to MI in deep lattice.

We conclude that the SF phase is always fragmented in the shallow lattice, introducing long-range dipolar interaction, fragmentation is enhanced. The effect of long-range tail is observed only when the lattice is very weak and the interaction dominates.

For deep lattice, the physics is determined by the lattice depth and all many-body measures become identical for the fragmented Mott phase irrespective of the range of interaction. We are unable to distinguish the full blown three-fold fragmented states of contact interaction from those with dipolar interaction. It needs further investigation of one-body and two-body correlation functions. We also perform calculations with various λ_0, but do not observe any new phases. With increase in λ_0, fragmentation is enhanced and transition to Mott localization in deep lattice happens faster. For very strong dipolar interaction, true Mott localization happens even in vanishing lattice.

4.2. Delocalization in Fock space

The pathway from fragmented SF to incomplete fragmented Mott state to one-third fragmented Mott state can be well understood by the "partial delocalization to complete delocalization" in the many boson Fock space. In Fig. 2, we plot the expansion coefficients $|C_{\vec{n}}|^2$ as a function of the index of the basis states for various choices of lattice depth, V_0(in units of E_r) = 0.3, 0.5, 1.0,2.0. We consider only weak lattice where the effect of dipolar interaction is manifested and can be distinguished from the contact interaction. The left panel corresponds to contact interaction and the right panel corresponds to dipolar interaction. The index is determined based on the vector $\vec{n}$ through the mapping outlined in Ref. [57] and basically determines the dimension of the Hilbert space.

For $V_0 = 0.3E_r$, with contact interaction, only one nonzero element of $\{C_{\vec{n}}\}$ occupy a very small portion of Hilbert space, we refer it to a localized many-body state. Localized states closely resemble a mean-field description, where only a single coefficient would play the significant role. When the coefficient is distributed over significant number of indices, the corresponding many-body state is referred to a delocalized state. With increase in lattice depth, several significant $\{C_{\vec{n}}\}$ contributes and the initial localized state exhibits delocalization. In contrary, for the dipolar interaction, many significant $\{C_{\vec{n}}\}$ contribute and the many-body state is already delocalized for $V_0 = 0.3E_r$ and becomes completely delocalized with increase in lattice depth. Thus the fragmented SF (QSF) and incomplete fragmented Mott (QMI) exhibit partial to complete delocalization in the Fock space.

4.3. One- and two-body correlation function

The one-body and two-body Glauber's correlation functions are evaluated accordingly Eqs. (8) and (9)—they provide spatially resolved information about the coherence of atoms. The structure of $|g^{(1)}|^2$ with varying lattice depth gives an intuitive picture of the mechanism behind the excited fragmentation and also the underlying correlation in the complex many-body phases as observed in the vanishing and weak lattices. It also measures the proximity of the many-body state to a product of uncorrelated mean-field states for a fixed coordinate (x, x'). Fig. 3 shows a plot of $|g^{(1)}(x, x')|^2$ for various shallow lattice. The left column corresponds to contact interaction and the right column corresponds to dipolar interaction. For $V_0 = 0.3E_r$, for contact interaction, the uniform bright diagonal exhibits strong diagonal correlation only. It has no structure, and the isolated confinement of atoms in three distinct wells is not observed. Thus it is not a Mott phase although diagonal correlation is exhibited. The one-body correlation function also quantifies the off-diagonal correlation ($x \neq x'$). In the scale of diagonal correlation ($\simeq 100\%$), the off-diagonal correlation measures $\simeq 40\%$ all throughout the lattice. It signifies that this is a very complex many-body phase intermediate to superfluid and Mott phase. The complexity is due to interplay between strong interaction and correlation, the effect of lattice is negligible. For dipolar interaction, due to long-range repulsion, we observe strong diagonal correlation and close to vanishing off-diagonal correlation even in such shallow lattice. With gradual increase in lattice depth, for contact interaction, Mott localization starts to be seen at the cost of off-diagonal correlation. For dipolar interaction, the three distinct lobes across the diagonal exhibits a clear signature of loss of inter-well correlation while maintaining intra-well correlation which characterizes the three-fold fragmented Mott phase.

Next, we analyze the two-body correlation function $g^{(2)}(x', x, x', x) = g^{(2)}(x, x')$ for the same set of lattice depth potential as chosen earlier for the study of one-body correlation and plot it in Fig. 4. The left column corresponds to contact interaction and the right column is for the dipolar interaction. For a perfect superfluid phase (when bosons are weakly interacting), $g^{(2)}(x, x') \simeq 1$ for all x and x'–it infers that both the intra-well as well as inter-well coherence are maintained. For a Mott phase (deep lattice), $g^{(2)} \simeq 1$ at the off-diagonal part and $g^{(2)} \simeq 0$ along the diagonal clearly exhibits Mott localization. However, strongly interacting bosons in very weak lattices exhibit interesting structures both along the diagonal and off-diagonal. For vanishingly small lattice depth when the phase is fragmented superfluid, $g^{(2)}$ is extinguished along the diagonal, but localization effect is absent; off-diagonal correlation is maintained across the lattice. Now we gradually increase the lattice depth; the diagonal part develops a structure called "correlation hole" or "antibunching effect". Two particles can never be simultaneously found in the same well due to strong repulsion — this is termed as antibunching effect. The state is the incomplete fragmented Mott phase (QMI). Thus the fragmented superfluid and the incomplete fragmented MI both exhibit extinction of diagonal two-body correlation due to the antibunching effect, but the diagonal of the QSF phase is structureless whereas the QMI phase has the clear signature of correlation hole. For dipolar interaction, the correlation hole becomes distinct and the three brown lobes clearly distinguish three correlation holes (see Fig. 4).

Fig. 5 shows the local two-body density-density correlation $g^{(2)}(0, 0)$ as a function of lattice depth only in the regime of vanishing small and weak lattices. In the case of significant repulsive interactions, the bosons exhibit a tendency to repel each other, leading to a near-zero value for the second-order correlation function at $x = 0$ and $x' = 0$. A similar outcome is observed in the Mott Insulator phase, where each boson occupies a distinct well, resulting in an ideal Mott-Insulator state with $g^{(2)}(0, 0)$ precisely equals to zero. For contact interaction, in the vanishing lattice ($V_0 = 0.3E_r$), we observe $g^{(2)}(0, 0) \simeq 0.25$, thus the system exhibits a nonvanishing two-body local correlation. As we increase the lattice depth, $g^{(2)}(0, 0)$ gradually decreases but does not reach to $g^{(2)}(0, 0) \simeq 0$. It quantifies that the phase is indeed a quasi Mott phase, for contact interaction true Mott phases are not observed in shallow lattice. As we move to larger lattice depths, the system enters the Mott insulator (MI) phase, where $g^{(2)}(0, 0)$ becomes exactly zero (not

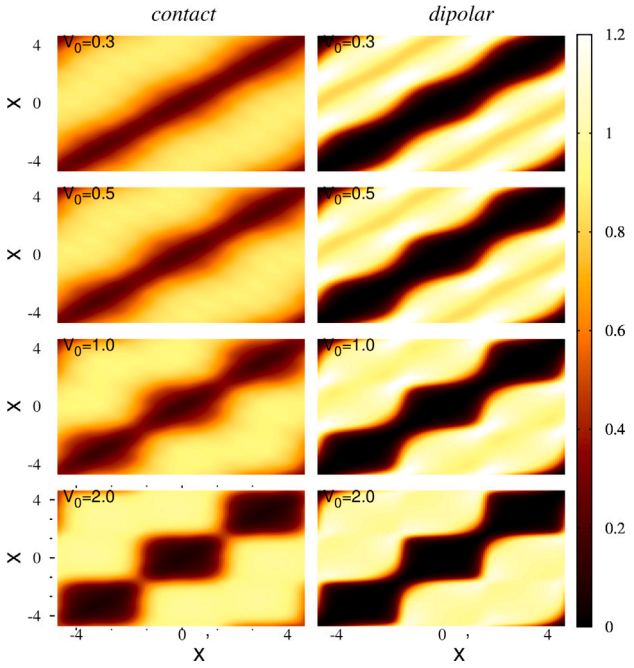

Fig. 4. Second-order coherence of fragmented SF (QSF), incomplete fragmented MI (QMI). The normalized second-order correlation function $g^{(2)}(x, x')$ is plotted for various lattice depth. Left column corresponds to contact interaction and the right column corresponds to dipolar interaction. A strong interplay between correlation and lattice effect is observed. A strong antibunching effect is demonstrated even for very weak lattices when the lattice effect is subrelevent. With the increase in lattice depth, gradually the structure of the correlation hole is built up. For dipolar interaction, three distinct correlation holes with $g^{(2)} = 0$ along the diagonal exhibits complete Mott localization. For contact interaction the correlation holes are visible with $g^{(2)} \simeq 0$. All quantities are dimensionless. See text for further discussion.

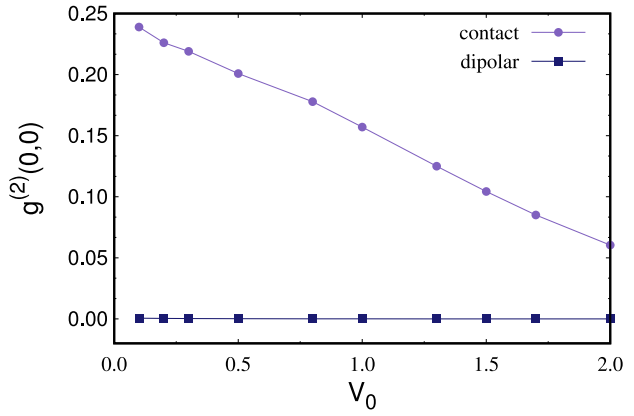

Fig. 5. Variation of the local two-body correlation function, $g^{(2)}(0, 0)$, with lattice depth in the shallow optical depth regime. For contact interaction, as the lattice depth increases, $g^{(2)}(0, 0)$ exhibits a smooth decrease, however true Mott phase is not reached. Whereas for long-range dipolar interaction, $g^{(2)}(0, 0)$ is consistently zero showing a true Mott phase in shallow lattice. Further details are provided in the text. The quantity is dimensionless.

depicted in the figure). Whereas for long-range dipolar interaction, $g^{(2)}(0, 0)$ is zero consistently due to long-range repulsion. It signifies that true Mott phase is reached in shallow lattice due to the long-range repulsion in the dipolar interaction.

The nonlocal density-density correlation $g^{(2)}(0, x)$ is plotted in Fig. 6. Due to a special symmetry in position space on either side of $x = 0$, we opt to plot only one half ($x > 0$) for various lattice depths. For contact interaction, at $x = x' = 0$, the local correlation remains consistently low, approaching zero due to strong repulsive interaction; the value is smaller for larger lattice depth as expected. The second-order non local correlation function $g^{(2)}(0, x)$ consistently increases and peaks around $x \approx 3.14$. This is significant because in a lattice with periodicity π, the minimum of the next lattice site aligns with $x \approx 3.14$. Considering three

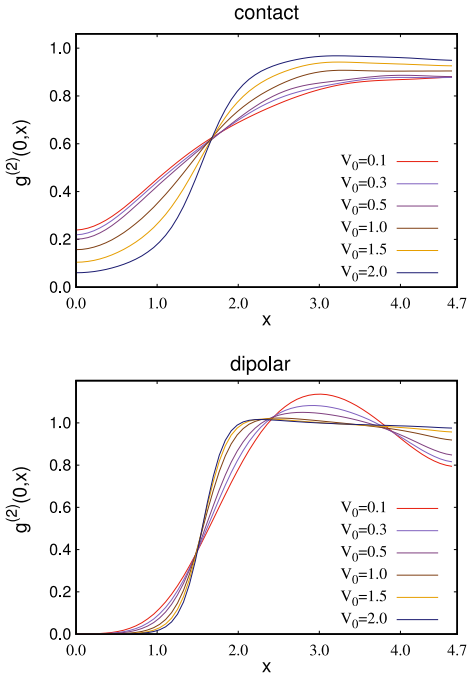

Fig. 6. Nonlocal density-density correlation at various lattice depths in the shallow lattice depth regime. For contact interaction, initially, $g^{(2)}(0,0)$ exhibits a low value near zero, gradually increases, and peaks around $x \sim 3.14$. This figure illustrates the persistence of two-body correlation with the neighboring lattice site and loss of two-body correlation within the lattice. For long-range dipolar interaction, $g^{(2)}(0,x) \simeq 0$ till $x = 1.0$ which exhibits the effect of long repulsive tail. Then it steeply increases and reaches to uncorrelated value. The quantity is dimensionless. Additional details can be found in the text.

lattice sites, $g^{(2)}(0,x)$ exhibits a high value around $x \approx 3.14$, indicating strong second-order correlations between adjacent sites. Moreover, the values of $g^{(2)}(0, x \approx 3.14)$ are higher for larger V_0. This highlights the combined influence of repulsive interaction and lattice depth in weak optical lattice. Thus, $g^{(2)}(0,x)$ serves as a valuable metric for studying the transition from quasi-superfluid (QSF) to quasi-Mott insulator (QMI) phase. For long-range dipolar interaction $g^{(2)}(0,x) \simeq 0$ for vanishing lattice, then steeply increases and attains a maximum at $x \simeq 3.14$, before it reaches the uncorrelated value $g^{(2)}(0,x) \simeq 1$.

4.4. Measures of information entropy

Many-body information entropy is another useful quantity for further characterization of complex many-body phases. We exemplify the entropy measure with the fragmentation. We calculate the occupation entropy S_n by the eigenvalues of the reduced one-body density matrix (Eq. (10)). We plot S_n as a function of lattice depth in Fig. 7 both for contact and dipolar interaction. As occupation entropy is obtained from the natural occupation, it is always zero for the mean-field picture, when there is only one natural occupation. We find, for a very weak lattice, when the many-body state is already fragmented, several natural orbitals contribute, and S_n has a significant value. With the increase in lattice depth, the many-body state gradually approaches one-third fragmentation–S_n saturates. We make a comparison between the saturation values of entropy and the prediction of the Gaussian orthogonal ensemble of random matrices (GOE) [55]. For the occupation entropy, the GOE analog is obtained by setting $n_i = \frac{N}{M}$ and $S_n^{GOE} = \ln(M)$. For a three-fold fragmented state, the lowest three natural orbitals contribute, thus $M = 3$ and $S_n^{GOE} = 1.09$ which is the saturation value as shown in Fig. 7. For contact interaction, the initial value of S_n is nonzero which signifies a fragmented phase. With increase in lattice depth, S_n increases as other orbitals contribute. Finally at large lattice depth when the system enters a true Mott phase, it exhibits three-fold fragmentation and S_n saturates to GOE prediction. For dipolar interaction, the superfluid in shallow lattice is strongly fragmented and the initial value of S_n is 1.23, which is higher than GOE prediction. In Fig. 1(b), it is already shown that although three natural orbitals significantly contribute, there is also small contribution from fourth and fifth orbitals, which has made S_n greater than GOE estimate. With gradual increase in lattice depth, S_n slowly decreases as the system leads to three-fold fragmented Mott state, S_n saturates to GOE prediction.

4.5. Coherence in incommensurate lattice

In this section, we present the results for two-body correlation for incommensurate filling, the incommensurate fraction of particles induces incomplete localization and a true Mott-insulator state is absent. We present results only for contact interaction.

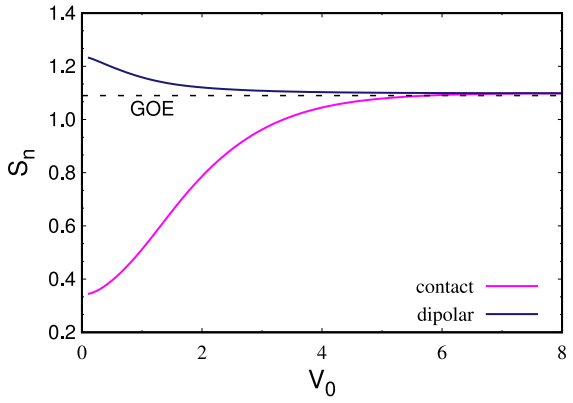

Fig. 7. Plot of occupation entropy as a function of lattice depth V_0, both for contact and dipolar interaction. For contact interaction, the system has significant entropy as the many-body state is fragmented and with increase in large lattice depth when the system makes a transition to a three-fold fragmented Mott phase, S_n saturates to GOE prediction. For dipolar interaction, in the vanishing lattice, the system is strongly fragmented SF, S_n is significantly higher than GOE prediction. With increase in lattice depth as 3-fold fragmentation happens, S_n decreases and reach to GOE estimate. All quantities are dimensionless. See the text for additional discussion.

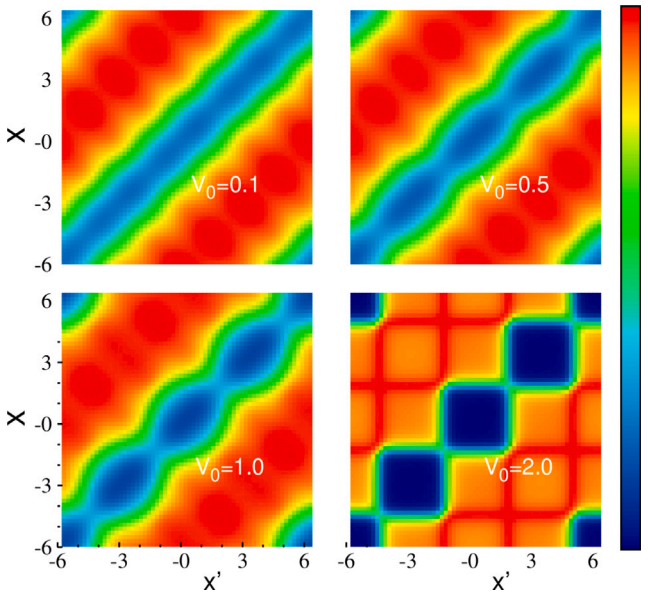

Fig. 8. Second-order coherence for four wells and three particles with $\lambda_0 = 1.05$, in shallow lattice of varying lattice depth. Distinct correlation holes become evident when $V_0 = 2.0E_r$. However the loss of off-diagonal correlation exhibits the effect of delocalization. All quantities are dimensionless.

We consider two cases of ν noninteger. For $\nu < 1$, we consider $N = 3$ bosons are in $S = 4$ lattice sites. The interatomic interaction is kept same as $\lambda_0 = 1.05$ and results for two-body coherence is presented in Fig. 8 for specific cases of lattice depth. In this case, as one extra site is always available, the one-particle density does not pull to have an equal site occupation. Due to repulsive interaction, the particles spread away from the center lattice. In Fig. 8, for $V_0 = 0.1E_r$, the diagonal part exhibits some extinction of correlation although structure of correlation hole is not seen, whereas the off-diagonal part exhibits two-body correlation as expected. With increase in lattice depth, the diagonal of two-body correlation exhibits correlation hole and at the same time, the off-diagonal correlation is reduced.

In Fig. 9, we plot the two-body coherence for $\nu > 1$, $N = 6$ particles are in $S = 4$ lattice sites, thus a repulsive pair of particles exists on a localized background. Due to repulsive interaction of the two extra particle, one-body density is pushed to the outer wells. This extra pair of particles feels the intra-pair repulsive force and additionally feels the repulsive interaction with the localized background. On increase in lattice depth the intra-well structure of two spatially separated bosons becomes clear.

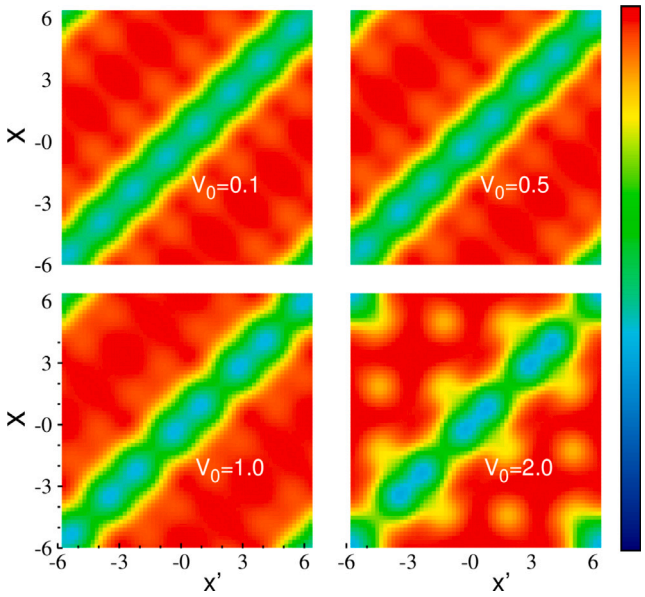

Fig. 9. Second-order coherence for four wells and six particles with $\lambda_0 = 1.05$, in shallow lattice of varying lattice depth. The localization of two extra particles happen in the outer wells. For $V_0 = 2.0$, intra-well repulsion exhibits spatially separated bosons in the doubly occupied wells. All quantities are dimensionless.

5. Conclusion

In conclusion, we have applied a numerically exact many-body approach, MCTDHB, to solve the many-body Schrödinger equation to study the ground states of strongly interacting bosons in vanishingly small and weak lattices. We explore the emergent phases: fragmented superfluid and incomplete fragmented Mott phases which are termed quasi superfluid (QSF) and quasi Mott (QMI) phases. In the usual notion of the Bose Hubbard picture: the superfluid is characterized by a single orbital occupation that exhibits correlation across the lattice; whereas the Mott phase is characterized by complete localization in each site and thus extinction of inter-well correlation. However, in the many-body perspective, we find some intermediate phases that cannot be explored by mean-field theory or the Bose-Hubbard model. To differentiate between these recently discovered phases, we have utilized fragmentation as a key metric. Additionally, we have introduced an order parameter based on the eigenvalues of the reduced one-body density matrix, providing another effective tool for investigating these distinct phases. Our analysis has been further bolstered by comprehensive study of one- and two-body correlations, as well as information entropy. Fragmentation is the figure of merit to distinguish the fragmented superfluid phase from the traditional superfluid phase as well as the incomplete fragmented Mott phase from the traditional Mott phase. We study the complete pathway of transition to the Mott phase for deep lattices. The measures of several information entropy clearly distinguish the limitation of mean-field physics. The order parameter and the structure of one and two-body coherence are utilized as the key markers to study the new phases. The structures evident in one- and two-body coherence serve as robust indicators, facilitating an understanding different intermediate phases in optical lattice. The fragmented many-body phases in shallow lattice are also studied for the long-range dipolar interaction. We observe that all the many-body features for quasi phases with contact interaction become distinct due to long-range repulsive tail in the dipolar interaction. In comparison with contact interaction, we conclude the possibility of true Mott phase for dipolar bosons even in extremely weak lattice. We also study the two-body coherence for contact interaction with incommensurate filing. We observe very rich structure in the coherence in absence of a true Mott insulator phase as there is always a superfluid fraction at the background of Mott phase.

We work with a finite ensemble of few bosons but this provides an experimental bottom-up access to the many-body physics. The dynamic evolution from the superfluid (SF) phase to the Mott insulator (MI) phase has already been explored [30,45,47]. An immediate and open question in this line is to investigate how the system evolves when subjected to a quench from the QSF to the QMI phase in the strong interaction regime. It would also be a challenging many-body calculation to study the stability of these intermediate phases in the presence of disorder.

CRediT authorship contribution statement

Subhrajyoti Roy: Writing – original draft, Visualization, Software, Data curation. **Rhombik Roy:** Writing – original draft, Visualization, Validation, Supervision, Methodology, Formal analysis, Conceptualization. **Arnaldo Gammal:** Writing – review & editing, Supervision, Investigation, Formal analysis, Conceptualization. **Barnali Chakrabarti:** Writing – review & editing, Writing – original draft, Visualization, Supervision, Software, Project administration, Methodology, Investigation, Formal analysis, Data

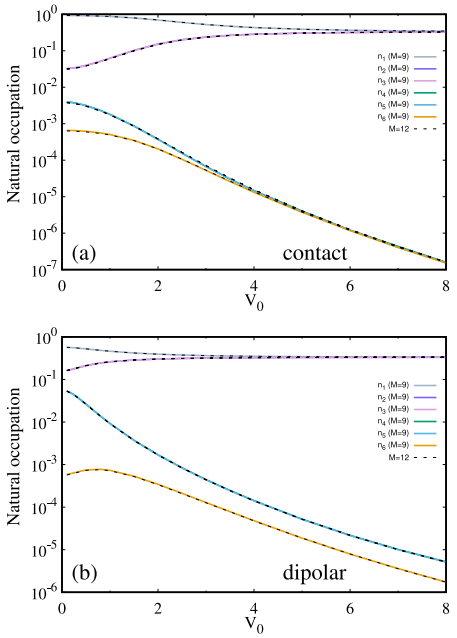

Fig. A.10. Orbital convergence analysis for unit filling scenarios. (a) Contact interaction case: Comparison of natural occupation of first three natural orbitals using varying numbers of time-dependent orbitals. (b) Dipolar interaction case: Comparison of natural occupation of first four natural orbitals for varying numbers of time-dependent orbitals. Calculations are done using $M = 9$ and $M = 12$ orbitals. Analysis indicates that $M = 9$ orbitals are sufficient for converge result.

curation, Conceptualization. **Budhaditya Chatterjee:** Writing – review & editing, Validation, Supervision, Methodology, Formal analysis.

Declaration of competing interest

The authors declare that they have no known competing financial interests or personal relationships that could have appeared to influence the work reported in this paper.

Data availability

Data will be made available on request.

Acknowledgments

A G acknowledges CNPq-Conselho Nacional de Desenvolvimento Científico e Tecnológico (Brazil) grant no. 306209/2022-0. B C acknowledges FAPESP grant Process No. 2023/06550-4.

Appendix. Numerical convergences

In this appendix, we examine the convergence of our results with respect to the number of time-adaptive orbitals. While the main text presents findings using $M = 9$ orbitals, we have conducted additional calculations using $M = 12$ orbitals to verify convergence. These calculations were performed for both contact and dipolar interactions, focusing on unit filling factor cases (three bosons in three wells). We have also checked convergence for incommensurate cases, but those results are not presented here.

Fig. A.10 illustrates the first three natural orbital occupations computed with $M = 9$, and $M = 12$ orbitals. For the contact interaction case, we observe that the occupations for $M = 9$ and $M = 12$ orbitals are overlapped for first six contributing occupations. From these observations, we conclude that $M = 9$ orbitals are sufficient to achieve converged results. In the case of dipolar interactions, we notice a more pronounced difference for calculations using $M = 6$ orbitals, indicates $M = 6$ is inadequate to describe the dipolar case (not shown). However, the results for $M = 9$ and $M = 12$ orbitals overlapped, confirming that $M = 9$ orbitals are sufficient for convergence in dipolar interaction scenarios as well. It is worth noting that despite larger depletion in this case, $M = 9$ orbitals still provide converged results. We have not presented results for other lower orbitals due to their very low occupation levels. Nevertheless, we have verified that these results are also converged. This comprehensive analysis ensures the reliability of our findings across different measured quantity for different lattice depth.

References

[1] I. Bloch, J. Dalibard, W. Zwerger, Many-body physics with ultracold gases, Rev. Modern Phys. 80 (2008) 885–964.
[2] A. Polkovnikov, K. Sengupta, A. Silva, M. Vengalattore, Colloquium: Nonequilibrium dynamics of closed interacting quantum systems, Rev. Modern Phys. 83 (2011) 863–883.
[3] H.U.R. Strand, M. Eckstein, P. Werner, Nonequilibrium dynamical mean-field theory for bosonic lattice models, Phys. Rev. X 5 (2015) 011038.
[4] M. Greiner, I. Bloch, O. Mandel, T.W. Hänsch, T. Esslinger, Exploring phase coherence in a 2d lattice of Bose-Einstein condensates, Phys. Rev. Lett. 87 (2001) 160405.
[5] S. Trotzky, Y.A. Chen, A. Flesch, I.P. McCulloch, U. Schollwöck, J. Eisert, I. Bloch, Probing the relaxation towards equilibrium in an isolated strongly correlated one-dimensional bose gas, Nat. Phys. 8 (2012) 325–330.
[6] M. Greiner, O. Mandel, T. Esslinger, T.W. Hänsch, I. Bloch, Quantum phase transition from a superfluid to a mott insulator in a gas of ultracold atoms, Nature 415 (39) (2002).
[7] M. Greiner, O. Mandel, T.W. Hansch, I. Bloch, Collapse and revival of the matter wave field of a Bose–Einstein condensate, Nature 419 (51) (2002).
[8] W.S. Bakr, A. Peng, M.E. Tai, R. Ma, J. Simon, J.I. Gillen, S. Fölling, L. Pollet, M. Greiner, Probing the superfluid–to–mott insulator transition at the single-atom level, Science 329 (2010) 547–550.
[9] D. Jaksch, C. Bruder, J.I. Cirac, C.W. Gardiner, P. Zoller, Cold bosonic atoms in optical lattices, Phys. Rev. Lett. 81 (1998) 3108–3111.
[10] L. Maciej, A. Sanpera, V. Ahufinger, Ultracold Atoms in Optical Lattices: Simulating Quantum Many-Body Systems, Oxford University Press, 2012.
[11] O. Dutta, M. Gajda, P. Hauke, M. Lewenstein, D.S. Lühmann, B.A. Malomed, T. Sowiński, J. Zakrzewski1, Non-standard hubbard models in optical lattices: a review, Rep. Progr. Phys. 78 (2015) 066001.
[12] E. Haller, R. Hart, M.J. Mark, G.D. Johann, M. Reichsöllner, M. Dalmonte, G. Pupillo, H.C. Nägerl, Pinning quantum phase transition for a luttinger liquid of strongly interacting bosons, Nature 466 (597) (2010).
[13] E. Haller, M. Gustavsson, M.J. Mark, J.G. Danzl, R. Hart, G. Pupillo, H.C. Nägerl, Realization of an excited, strongly correlated quantum gas phase, Science 325 (2009) 1224–1227.
[14] S. Coleman, Quantum Sine-Gordon equation as the massive thirring model, Phys. Rev. D 11 (2088) (1975).
[15] H.P. Büchler, G. Blatter, W. Zwerger, Commensurate-incommensurate transition of cold atoms in an optical lattice, Phys. Rev. Lett. 90 (2003) 130401.
[16] A. Lazarides, M. Haque, Strongly interacting one-dimensional bosons in optical lattices of arbitrary depth: From the Bose-Hubbard to the sine-gordon regime and beyond, Phys. Rev. A 85 (2012) 063621.
[17] G.E. Astrakharchik, K.V. Krutitsky, M. Lewenstein, F. Mazzanti, One-dimensional bose gas in optical lattices of arbitrary strength, Phys. Rev. A 93 (2016) 021605(R).
[18] G. Boéris, L. Gori, M.D. Hoogerland, A. Kumar, E. Lucioni, L. Tanzi, M. Inguscio, T. Giamarchi, C. D'Errico, G. Carleo, G. Modugno, L.S. Palencia, Mott transition for strongly interacting one-dimensional bosons in a shallow periodic potential, Phys. Rev. A 93 (2016) 011601(R).
[19] M. Rispoli, A. Lukin, R. Schittko, S. Kim, M.E. Tai, J. Léonard, M. Greiner, Quantum critical behaviour at the many-body localization transition, Nature 573 (2019) 385–389.
[20] M. Holten, L. Bayha, K. Subramanian, S. Brandstetter, C. Heintze, P. Lunt, P.M. Preiss, S. Jochim, Observation of cooper pairs in a mesoscopic two-dimensional fermi gas, Nature 606 (2022) 287–291.
[21] A.I. Streltsov, O.E. Alon, L.S. Cederbaum, General variational many-body theory with complete self-consistency for trapped bosonic systems, Phys. Rev. A 73 (2006) 063626.
[22] A.I. Streltsov, O.E. Alon, L.S. Cederbaum, Role of excited states in the splitting of a trapped interacting Bose-Einstein condensate by a time-dependent barrier, Phys. Rev. Lett. 99 (2007) 030402.
[23] O.E. Alon, A.I. Streltsov, L.S. Cederbaum, Unified view on multiconfigurational time propagation for systems consisting of identical particles, J. Chem. Phys. 127 (2007) 154103.
[24] O.E. Alon, A.I. Streltsov, L.S. Cederbaum, Multiconfigurational time-dependent Hartree method for bosons: Many-body dynamics of bosonic systems, Phys. Rev. A 77 (2008) 033613.
[25] A.U.J. Lode, Multiconfigurational time-dependent Hartree method for bosons with internal degrees of freedom: Theory and composite fragmentation of multicomponent bose-einstein condensates, Phys. Rev. A 93 (2016) 063601.
[26] E. Fasshauer, A.U.J. Lode, Multiconfigurational time-dependent Hartree method for fermions: Implementation, exactness, and few-fermion tunneling to open space, Phys. Rev. A 93 (2016) 033635.
[27] A.U.J. Lode, L.B. Lévêque, A.I. Streltsov, O.E. Alon, Colloquium: Multiconfigurational time-dependent Hartree approaches for indistinguishable particles, Rev. Modern Phys. 92 (2020) 011001.
[28] R. Lin, P. Molignini, L. Papariello, M.C. Tsatsos, C. Lévêque, S.E. Weiner, E. Fasshauer, R. Chitra, Mctdh-x: The multiconfigurational time-dependent Hartree method for indistinguishable particles software, Quantum Sci. Technol. 5 (2020) 024004.
[29] A.U.J. Lode, M.C. Tsatsos, E. Fasshauer, S.E. Weiner, R. Lin, L. Papariello, P. Molignini, M. Lévêque, J. Xiang, S. Dutta, Y. Bilinskaya, MCTDH-x: The MultiConfigurational time-dependent hartree method for indistinguishable particles software, 2024, URL http://ultracold.org.
[30] M.P.A. Fisher, P.B. Weichman, G. Grinstein, D.S. Fisher, Boson localization and the superfluid-insulator transition, Phys. Rev. B 40 (1989) 546–570.
[31] L. Cao, S. Krönke, O. Vendrell, P. Schmelcher, The multi-layer multi-configuration time-dependent Hartree method for bosons: Theory, implementation, and applications, J. Chem. Phys. 139 (2013) 134103.
[32] U. Manthe, A multilayer multiconfigurational time-dependent Hartree approach for quantum dynamics on general potential energy surfaces, J. Chem. Phys. 128 (2008) 164116.
[33] M. Beck, A. Jäckle, G. Worth, H.D. Meyer, The multiconfiguration time-dependent Hartree (mctdh) method: a highly efficient algorithm for propagating wavepackets, Phys. Rep. 324 (2000) 1–105.
[34] H. Wang, M. Thoss, Multilayer formulation of the multiconfiguration time-dependent Hartree theory, J. Chem. Phys. 119 (2003) 1289–1299.
[35] S.K. Haldar, O.E. Alon, Impact of the range of the interaction on the quantum dynamics of a bosonic josephson junction, Chem. Phys. 509 (2018) 72–80, High-dimensional quantum dynamics (on the occasion of the 70th birthday of Hans-Dieter Meyer).
[36] H. Wang, Multilayer multiconfiguration time-dependent Hartree theory, J. Phys. Chem. A 119 (2015) 7951–7965.
[37] A. Bhowmik, O.E. Alon, Longitudinal and transversal resonant tunneling of interacting bosons in a two-dimensional josephson junction, Sci. Rep. 12 (627) (2022).
[38] D.J. Haxton, C.W. McCurdy, Two methods for restricted configuration spaces within the multiconfiguration time-dependent Hartree-fock method, Phys. Rev. A 91 (2015) 012509.
[39] L. Cao, V. Bolsinger, S.I. Mistakidis, G.M. Koutentakis, S. Krönke, J.M. Schurer, P. Schmelcher, A unified ab initio approach to the correlated quantum dynamics of ultracold fermionic and bosonic mixtures, J. Chem. Phys. 147 (2017) 044106.
[40] C. Lévêque, L.B. Madsen, Time-dependent restricted-active-space self-consistent-field theory for bosonic many-body systems, New J. Phys. 19 (2017) 043007.
[41] R. Lin, C. Georges, J. Klinder, P. Molignini, M. Büttner, A.U.J. Lode, R. Chitra, A. Hemmerich, H. Keßler, Mott transition in a cavity-boson system: A quantitative comparison between theory and experiment, SciPost Phys. 11 (30) (2021).

[42] J.H.V. Nguyen, M.C. Tsatsos, D. Luo, A.U.J. Lode, G.D. Telles, V.S. Bagnato, R.G. Hulet, Parametric excitation of a Bose-Einstein condensate: From faraday waves to granulation, Phys. Rev. X 9 (2019) 011052.
[43] A.U.J. Lode, K. Sakmann, O.E. Alon, L.S. Cederbaum, A.I. Streltsov, Numerically exact quantum dynamics of bosons with time-dependent interactions of harmonic type, Phys. Rev. A 86 (2012) 063606.
[44] A.U.J. Lode, B. Chakrabarti, V.K.B. Kota, Many-body entropies, correlations, and emergence of statistical relaxation in interaction quench dynamics of ultracold bosons, Phys. Rev. A 92 (2015) 033622.
[45] S. Bera, R. Roy, A. Gammal, B. Chakrabarti, B. Chatterjee, Probing relaxation dynamics of a few strongly correlated bosons in a 1d triple well optical lattice, J. Phys. B: At. Mol. Opt. Phys. 52 (2019) 215303.
[46] R. Roy, A. Gammal, M.C. Tsatsos, B. Chatterjee, B. Chakrabarti, A.U.J. Lode, Phases, many-body entropy measures, and coherence of interacting bosons in optical lattices, Phys. Rev. A 97 (2018) 043625.
[47] R. Roy, C. Lévêque, A.U.J. Lode, A. Gammal, B. Chakrabarti, Fidelity and entropy production in quench dynamics of interacting bosons in an optical lattice, Quant. Rep. 1 (2019) 304–316.
[48] R. Roy, B. Chakrabarti, A. Trombettoni, Quantum dynamics of few dipolar bosons in a double-well potential, Eur. Phys. J. D 76 (2022) 215303.
[49] S. Bera, R. Roy, B. Chakrabarti, How to distinguish fermionized bosons from noninteracting fermions through one-body and two-body density, AIP Conf. Proc. 2072 (2019) 020011.
[50] R. Roy, B. Chakrabarti, N.D. Chavda, M.L. Lekala, Information theoretic measures for interacting bosons in optical lattice, Phys. Rev. E 107 (2023) 024119.
[51] R. Roy, B. Chakrabarti, A. Gammal, Out of equilibrium many-body expansion dynamics of strongly interacting bosons, SciPost Phys. Core 6 (073) (2023).
[52] S.E. Massen, C.P. Panos, Universal property of the information entropy in atoms, nuclei and atomic clusters, Phys. Lett. A 246 (1998) 530.
[53] S.E. Massen, C.P. Panos, A link of information entropy and kinetic energy for quantum many-body systems, Phys. Lett. A 280 (65) (2001).
[54] S.E. Massen, C. Moustakidis, C.P. Panos, Comparison of the information entropy in fermionic and bosonic systems, Phys. Lett. A 299 (131) (2002).
[55] V.K.B. Kota, R. Sahu, Single-particle entropy in (1+2)-body random matrix ensembles, Phys. Rev. E 66 (2002) 037103.
[56] M. Rigol, Quantum quenches in the thermodynamic limit, Phys. Rev. Lett. 112 (2014) 170601.
[57] A.I. Streltsov, O.E. Alon, L.S. Cederbaum, General mapping for bosonic and fermionic operators in fock space, Phys. Rev. A 81 (2010) 022124.